ORIGINAL RESEARCH

Integrated Network Pharmacology and Experimental Validation Approach to Investigate the Mechanisms of Radix Rehmanniae Praeparata - Angelica Sinensis - Radix Achyranthis Bidentatae in Treating Knee Osteoarthritis

Lang Liu[1,]*, Binghua Zhang[1,]*, Zhenwei Zhou[2], Jie Yang[1], Ailin Li[1], Yongji Wu[1], Zeyu Peng[1], Xiangyan Li [2], Zhonghua Liu[3], Xiangyang Leng[1], Changwei Zhao[4], Haisi Dong[2], Wenhai Zhao[4]

[1]College of Traditional Chinese Medicine, Changchun University of Chinese Medicine, Changchun, People's Republic of China; [2]Northeast Asia Institute of Traditional Chinese Medicine, Changchun University of Chinese Medicine, Changchun, People's Republic of China; [3]Department of Orthopaedics, The Third Affiliated Hospital of Changchun University of Chinese Medicine, Changchun, People's Republic of China; [4]Affiliated Hospital of Changchun University of Chinese Medicine, Changchun University of Chinese Medicine, Changchun, People's Republic of China

*These authors contributed equally to this work

Correspondence: Haisi Dong, Northeast Asia Institute of Traditional Chinese Medicine, Changchun University of Chinese Medicine, Changchun, Jilin, 130117, People's Republic of China, Tel/Fax +86 431-18604361976, Email adonghaisi@163.com; Wenhai Zhao, Affiliated Hospital of Changchun University of Chinese Medicine, Changchun University of Chinese Medicine, Changchun, Jilin, 130021, People's Republic of China, Tel/Fax +86 431-86177836, Email zwh9899@163.com

Background: Knee osteoarthritis (KOA) is a persistent degenerative condition characterized by the deterioration of cartilage. The Chinese herbal formula Radix Rehmanniae Praeparata- Angelica Sinensis-Radix Achyranthis Bidentatae (RAR) has often been used in effective prescriptions for KOA as the main functional drug, but its underlying mechanism remains unclear. Therefore, network pharmacology and verification experiments were employed to investigate the impact and mode of action of RAR in the treatment of KOA.

Methods: The destabilization of the medial meniscus model (DMM) was utilized to assess the anti-KOA effect of RAR by using gait analysis, micro-computed tomography (Micro-CT), and histology. Primary chondrocytes were extracted from the rib cartilage of a newborn mouse. The protective effects of RAR on OA cells were evaluated using a CCK-8 assay. The antioxidative effect of RAR was determined by measuring reactive oxygen species (ROS), superoxide dismutase (SOD), and glutathione (GSH) production. Furthermore, network pharmacology and molecular docking were utilized to propose possible RAR targets for KOA, which were further verified through experiments.

Results: In vivo, RAR significantly ameliorated DMM-induced KOA characteristics, such as subchondral bone sclerosis, cartilage deterioration, gait abnormalities, and the degree of knee swelling. In vitro, RAR stimulated chondrocyte proliferation and the expression of Col2a1, Comp, and Acan. Moreover, RAR treatment significantly reduced ROS accumulation in an OA cell model induced by IL-1β and increased the activity of antioxidant enzymes (SOD and GSH). Network pharmacology analysis combined with molecular docking showed that Mapk1 might be a key therapeutic target. Subsequent research showed that RAR could downregulate Mapk1 mRNA levels in IL-1β-induced chondrocytes and DMM-induced rats.

Conclusion: RAR inhibited extracellular matrix (ECM) degradation and oxidative stress response via the MAPK signaling pathway in KOA, and Mapk1 may be a core target.

Keywords: knee osteoarthritis, RAR, cartilage degeneration, network pharmacology, Mapk1

Introduction

Osteoarthritis (OA) is a degenerative bone and joint disease that affects bone, cartilage, and the synovium.[1,2] KOA is the most common form of OA. Chronic pain and disability associated with KOA often cause anxiety and depression in patients, negatively impacting their quality of life.[3,4] International recommendations recommend nonsteroidal anti-inflammatory medicines (NSAIDs) as the first therapy for KOA; however, it is important to be aware of the potential negative effects of these medications.[5,6]

Cartilage matrix degradation mediated by inflammation and oxidative stress are the most important pathological changes.[7,8] IL-1β is a significant proinflammatory cytokine in OA that is capable of causing severe inflammatory responses and cartilage matrix breakdown.[9,10] The synovial fluid of OA patients has been shown to contain increased amounts of IL-1β.[11] The buildup of inflammatory mediators causes mitochondrial DNA (mtDNA) damage and reactive oxygen species (ROS) overproduction, along with intrinsic catabolic reactions in chondrocytes, resulting in an imbalance between cartilage repair and destruction, which is a hallmark of OA.[12–14] In addition, One such element that can activate pro-inflammatory pathways and contribute to articular chondrocyte degeneration is oxidative stress.[15] Increased oxidative stress, along with increased ROS generation in articular chondrocytes, may lead to an inflammatory response.[16] Through their role as second messengers, ROS can primarily induce OA by activating the ROS/mitogen-activated protein kinase (MAPK) pathway.[17] Stressful conditions such as inflammation or elevated ROS levels cause chondrocyte anabolism to decrease, while catabolism increases, hastening the onset of OA.[18] As translational therapeutics, multifaceted techniques, such as ROS clearance and inflammation reduction under stressful conditions, show promise.[19,20]

Herbal pharmaceutically active components, which have comprehensive therapeutic effects and few side effects on the human body, have particular effects and great development potential for lowering oxidative stress and treating KOA.[21] Therefore, identifying safe and effective potential traditional Chinese medicine (TCM) drugs has become a hot topic in KOA prevention and treatment. KOA is classified as "arthralgia (Bi) syndrome" in TCM. The primary reason is a deficiency of kidney Qi inside the human body, along with the influence of malevolent Qi from the external environment. According to this principle, a wide variety of TCM formulas have been developed. The traditional Chinese medicinal compound known as Radix Rehmanniae Praeparata- Angelica sinensis-Radix Achyranthis Bidentatae (RAR) are usually as monarch herbal medicine plays a principal role in therapeutic effect in the traditional formula for OA. For instance, the Du Huo Ji Sheng Tang (DHJST), a well-known formula for the clinical treatment of KOA in China for more than a thousand years, and contains RAR.[22] Our previous research also revealed that the Chinese herbal formula BuShen JianGu Fang (BSJGF) has a significant effect on cartilage protection, and Radix Rehmanniae Praeparata and Radix Achyranthis Bidentatae as monarch herbal medicine plays a principal role in therapeutic effect.[23] The ancient Chinese medicine "Materia Medica" records that RAR has historic therapeutic effectiveness in stimulating blood circulation, invigorating Qi, healing blood stasis, and treating the symptoms of joint pain and severe back pain. According to earlier research, Radix Rehmanniae Praeparata has many biological effects, such as anticancer and anti-inflammatory effects, that can help treat bone illnesses such as OA.[24,25] Angelica Sinensis possesses anti-inflammatory and antiapoptotic properties and has been widely used in TCM for treating various diseases, such as inflammation, infections, and OA.[26,27] The Chinese herb Radix Achyranthis Bidentatae was reported to have antioxidative and anti-inflammatory effects.[28] However, the molecular mechanism by which RAR treats KOA remains unknown, limiting its therapeutic use.

Network pharmacology is recognized as a new research method for studying complex network relationships between components, potential targets, correlations with diseases, and other TCM information based on databases.[29,30] Therefore, the purpose of the present study was to determine the possible targets and mechanisms of RAR in the treatment of KOA by combining network pharmacology with experimental techniques, thus providing an experimental basis for RAR treatment of OA. Figure 1 displays the flow chart.

Materials and Methods
Preparation of RAR

RAR was obtained from the Affiliated Hospital of Changchun University of Chinese Medicine. Radix Rehmanniae Praeparata (30 g), Radix Achyranthis Bidentatae (20 g), and Angelica Sinensis (10 g) were mixed with 10 times distilled
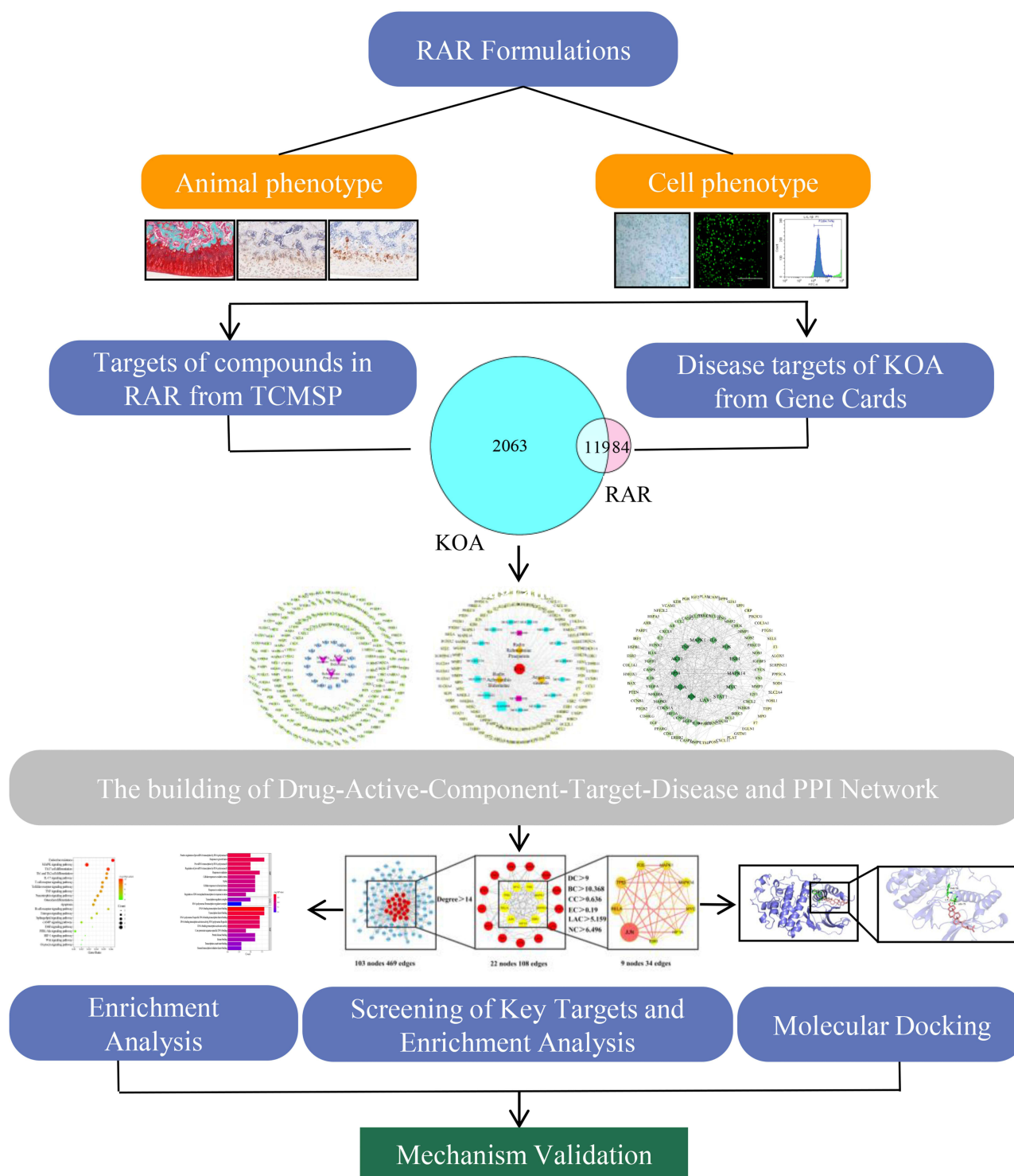
Figure 1 Process flowchart for research analysis.

water to obtain the RAR water extract. This was followed by 1 h of boiling. The aforementioned technique was performed three times after collecting the aqueous extract. The filtrate was combined and concentrated by a rotary evaporator twice. After 24 h, the concentrated liquid was dried in a freeze dryer (FDU-1100, Japan) for 72 h.

Animals

Eight-week-old male Sprague Dawley rats were acquired from Liaoning Changsheng Biotechnology Co., Ltd. (Certificate number: SCXK (Liao) 2020–0001). The rats were raised in an environment with sufficient light as well as adequate temperature and humidity. The Changchun University of Chinese Medicine Animal Care and Use Committee authorized and monitored the research (No. ccucm-2024218).

After adaptive feeding for seven days, 60 rats were randomly assigned to six groups: the sham group (n=10), model group (n=10), RAR low group (n=10), RAR medium group (n=10), RAR high group (n=10), and positive control (PC) drug group (n=10). Celecoxib is one of the most effective medications for treating osteoarthritis; it was officially included in the nonsurgical treatment guidelines issued in 2019 by the Osteoarthritis Research Society International Organization (OARSI) and was selected as a PC drug.[31] Then, the rats in the model and RAR groups underwent DMM surgery to establish the OA model.[32] A similar surgery was performed on the rats in the sham group, but the articular capsule was not exposed. In brief, the rats were anesthetized intraperitoneally with 3% pentobarbital sodium (40 mg/kg) prior to surgery. The right knee joint was cleaned three times with iodophor before being subjected to a medial capsular incision. According to the common clinical doses, the recommended dose for RAR is 0.57 g/kg. Based on the animal dose conversion table and the recovery rate of drugs, it was concluded that the administered dose in rats should be 1.5 g/kg. The weight of the rats used in the experiments was usually approximately 200 g; consequently, 300 mg/mL was used for the medium-dose group, 150 mg/mL was used for the low-dose group, and 600 mg/mL was used for the high-dose group. Following surgery, the PC rats were orally administered celecoxib (30 mg/kg) for four weeks.

Gait Analysis

A DigiGait Imaging System (Boston, USA) was used for gait analysis. Briefly, the machine's video camera captured photos of the four paws. The rats ran for up to 60s on a transparent flat treadmill at a pace of 25 cm/s. The analysis phase was 6 s long. DigiGait picture analysis software automatically assessed stance width, pose time, paw weight, and paw area.

Micro-Computed Tomography (Micro-CT) Scan

The rats were euthanized after four weeks of intervention, and the right knee was treated with 4% paraformaldehyde (Cat No. BL539A, Biosharp, China) solution for Micro-CT examination. A Skyscan 1174 desktop Micro-CT scanner was used to scan the right knee samples at 60 kV and 800 μA. The three-dimensional (3D) structure of the knee was reconstructed using N-Recon software. The CT-AN program was used to assess several trabecular bone indices, including the trabecular thickness (Tb.Th), trabecular bone volume fraction (BV/TV), and trabecular spacing (Tb.Sp).

Histological Evaluation and Immunohistochemistry (IHC)

Safranin-O-solid green staining was used to assess the deterioration of cartilage in each group. Tissue samples were decalcified in 10% EDTA and fixed in 4% paraformaldehyde for four weeks. Safranin-O-solid green stain was applied to the paraffin slices. Each group of sections was blocked with 3% hydrogen peroxide for 10 min and 5% BSA for 30 min for IHC analysis. Knee joints were fixed in 4% paraformaldehyde for four weeks, decalcified in EDTA decalcifying solution for two weeks, embedded in paraffin, and sectioned. The tissue slices were then exposed to monoclonal antibodies against Acan (Proteintech, MA5-42646, 1:200), Col2a1 (Proteintech, 28459-1-AP, 1:200), and Mapk1 (Proteintech, 13–6200, 1:100) overnight at 4 °C. A horseradish peroxidase-conjugated secondary antibody was used to boost the signal. Visualization was performed using 3.3-diaminobenzidine chromagen or 3-amino-9-ethylcarbazole (Solarbio, China). Images were recorded with an Olympus (Japan) optical microscope. The immunohistochemistry results were analyzed using ImageJ software.

RAR Bioactive Component and Molecular Target Screening

The Traditional Chinese Medicine Systems Pharmacology (TCMSP) Database (https://tcmsp-e.com/) was used to evaluate and construct all RAR components. Oral bioavailability $\geq$ 30% and drug-likeness $\geq$ 0.18 were the screening

parameters. Simultaneously, studies were conducted on treating KOA with RAR to supplement the unpredictable active ingredients by PubMed (https://www.ncbi.nlm.nih.gov/pubmed). The TCMSP database and the Universal Protein Resource (UniProt) database (https://www.uniprot.org/uniprot/) were used in combination to discover the probable target genes associated with each active component. Ultimately, the individual targets were merged, and any duplicates were removed to obtain the prospective target set of RAR. Furthermore, main active components were determined by HPLC-MS/MS analysis on the Q Exactive Orbitrap (Thermo Scientific, USA).

Searching for KOA-Related Targets

The keyword "Knee osteoarthritis" was employed to search and evaluate KOA-related targets in the GeneCards database (https://www.genecards.org/), Online Mendelian Inheritance in Man Database (OMIM) (http://www.omim.org/), DisGeNet database (https://www.disgenet.org/), Therapeutic Target Database (http://db.idrblab.net/ttd/), and DrugBank database (https://go.drugbank.com/). Then, the screening results were combined and replicated to obtain KOA-related gene sets. Finally, to clarify the interaction between RAR and KOA, drugs and disease targets were input into the online Venny tool (https://bioinfogp.cnb.csic.es/tools/venny/index.html) to generate a Venn diagram.

Construction of a "Drug-Active Component-Target-Disease" Network

A network called "drug-active component-target-disease" was constructed using the connections between medications, active components, gene symbols, and illnesses. The network was visually analyzed using the Cytoscape program (v3.9.0). The color and shape of the visual mesh were adjusted according to the degree values.

Protein-Protein Interaction (PPI) Network Construction and Key Target Identification

The PPI network was constructed by importing targets from the STRING database (https://string-db.org/cgi/input.pl), with the species set to "Homo sapiens". The minimum required interaction score was set to 0.900 after hiding discrete targets. The data were then visualized using the Cytoscape program. The topological features of the PPI network were examined using the network topology analysis plugin CytoNCA. Then, the key target for RAR activity against KOA was determined based on the degree centrality (DC), betweenness centrality (BC), eigenvector centrality (EC), closeness centrality (CC), network centrality (NC), and the local average connectivity-based method (LAC).

Gene Ontology (GO) and Kyoto Encyclopedia of Genes and Genomes (KEGG) Enrichment Analyses

The primary RAR pathways for treating KOA and the core targets of the PPI network were entered into the Metascape database (https://metascape.org/) for GO and KEGG pathway enrichment analyses to further understand the possible mechanism of the core target genes. Using the Bioinformatics platform (http://www.bioinformatics.com.cn/), GO and KEGG pathway data were displayed.

Molecular Docking

RAR small molecule chemical structures were downloaded from the PubChem database (https://pubchem.ncbi.nlm.nih.gov/), and core target protein 3D structures were downloaded from the RCSB PDB database (https://www.pdbus.org/), which were then imported into PyMol software for dehydration and ligand separation to prepare macromolecular receptors. AutoDock Tools was used to translate the files of the small molecule ligands and large molecule receptors to the PDBQT format, and the ligands and receptors were processed and docked with the AutoDock4 program. The docking findings were imported into PyMol software for visualization.

Isolation and Cultivation of Primary Chondrocytes

Rib chondrocytes were extracted from C57BL/6J mice (Changchun Yisi Laboratory Animal Technology Co., Ltd., China) and utilized to establish an OA cell model generated by IL-1β, as previously reported.[33] Primary chondrocytes were extracted by centrifugation at 1100 rpm for 10 min and then cultured in DMEM/F-12 media (Cat. No. 11–320-033,

Gibco, USA) supplemented with 1% streptomycin-penicillin (Cat. No. V900929, Sigma, USA) and 5% FBS (Cat. No. 10099141C, Thermo, USA).

Analysis of Chondrocyte Activity

Chondrocytes were plated at a density of 8×10^3 cells per well in 96-well plates. The effects of RAR on cell proliferation were measured using a CCK-8 test kit (Cat No. CA1210, Solarbio, China). The RAR concentrations were 0, 0.05, 0.1, 0.2, 0.4, 0.6, 0.8, 1.0, and 1.2 mg/mL. All cells were grown in a cell incubator at 37 °C and 5% CO_2. CCK-8 reagent was added for 1.5 h after 24 h, and the absorbance was measured at 450 nm.

Alcian Blue Staining

In this work, Alcian blue staining (Cat No. S0135, Bioss, China) was used to evaluate chondrocyte extracellular matrix phenotypic changes. After 15 min, the cells were fixed in a 4% paraformaldehyde solution. The fixed cells were stained with 1% Alcian blue solution for 2 h after being rinsed three times with phosphate-buffered saline. The stained cells were rinsed with phosphate-buffered saline before being observed using a gross camera and an Olympus Leica inverted optical microscope.

Detection of ROS

As previously described, a CytoFLEX flow cytometer (Beckman Coulter, USA) and a ROS detection kit (Cat No. S0033S, Beyotime, China) were used to detect ROS.[34] Pretreated chondrocytes were incubated with DCFH-DA in 24-well plates at 37 °C for 30 min for fluorescence examination. Images were taken, and fluorescence intensity was assessed after three washes.

Detection of SOD and GSH

Chondrocytes were obtained, and the levels of the lipid peroxidation-related indices GSH and SOD in cell extracts were individually assessed using the GSH and Oxidized Glutathione Disulfide (GSSG) Assay Kit (Cat No. S0053, Beyotime China) and the SOD activity assay kit (Cat No. S0101S, Beyotime, China).

Quantitative Real-Time PCR (qRT–PCR)

Total RNA was extracted from primary chondrocytes using TRIzol (Tiangen, China). A PrimeScript™ RT reagent kit (TaKaRa, Japan) was used to synthesize first-strand cDNA. We performed qRT-PCR using Bio-Rad equipment (Bio-Rad, USA) and TB GreenR Premix Ex TaqTMII (Cat No. RR820A, TaKaRa, Japan) to measure gene expression. To estimate the relative gene expression level, we used the $2^{-\Delta\Delta CT}$ method. The primers used in this section of the experiment are outlined in Table 1.

Statistical Analysis

All experimental data were evaluated using SPSS 20.0. All studies were conducted at least three times, and the data are presented as the mean ± standard deviation (SD). Pairwise comparisons were performed with an independent *t*-test, and group differences were examined using one-way analysis of variance. *P* values less than 0.05 indicated significant differences.

Results

RAR Ameliorates Abnormal Gait and Swelling in OA Rats

The present research employed gait analysis and a knee joint swelling test to determine whether RAR may improve the symptoms of KOA in a rat model. As displayed in Figure 2A, similar to the PC group, oral administration of RAR at doses of 150, 300, and 600 mg/mL significantly inhibited DMM-induced knee joint edema in rats in a dose-dependent manner; in particular, at 600 mg/mL, RAR significantly reduced knee joint edema on week 2. All animals in the DMM group initially showed a reduction in the plantar surface area of the right hind paw. However, from week 2, the 300 and 600 mg/mL and PC groups showed a measurable increase in the plantar surface area of the hind paw compared to that of the DMM group (Figure 2B). Afterward, the distance between the hind paws of DMM- and RAR-treated rats was

Table 1 Primer Sequences

Animal	Target Name	Forward Primers (5"-3")	Reverse Primers (5"-3")
Mouse	Rpl4	CAAAGCTCCCATTCGACCAG	TGGTCTGATGACCTGCCAAT
	Jun	CAACATGCTCAGGGAACAGG	GTTTGCAACTGCTGCGTTAG
	Rela	GCTCCTGTTCGAGTCTCCAT	GTGGCGATCATCTGTGTCTG
	Mapk1	AGAGTACGTAGCCACACGTT	TGGGAAGATAGGCCTGTTGG
	Col2a1	CAAGAAGGCCTTGCTCATCC	CCATCCTTCAGGGCAGTGTA
	Acan	TTGTCTGAATGGAGCCACCT	ACACAGGTTCCCTCTGTAGC
	Comp	ACGTGGGCTGGAAGGATAAA	GTGTCCAACACCACATTGCT
Rat	Rpl4	GTATGGCACTTGGCGTAAGG	AATCTTCTTGCGTGGTGCTC
	Jun	GAGTCTCAGGAGCGGATCAA	CTGTTCCCTGAGCATGTTGG
	Rela	ACATCCCTCAGCACCATCAA	TTGGTACCATGGCTGAGGAG
	Mapk1	AAACGCTGACTCCAAAGCTC	CAATGGGCTCATCACTTGGG
	Col2a1	ATGGTATTCCCGGAGCCAAA	CAGGTCCAGTCTCTCCCTTG
	Acan	GCTACCCTGATCCCTCATCC	GATGTCCTCTTCACCACCCA
	Comp	GAGTGACAGCGATGGTGATG	TCCTGGTCTTGGTCACTGTC

measured using the stride length test. At week 2 and beyond, the 300 and 600 mg/mL RAR-treated groups showed a significantly shorter difference in hind paw stride than the DMM group (Figure 2C). Compared with those in the sham group, the rats in the DMM group showed a decrease in paw area, paw weight, and time spent standing during the four weeks of treatment. In addition, stride length, paw area, paw weight, and standing time were increased in DMM rats after RAR administration (Figures 2D–G). Collectively, these findings suggest that RAR has a therapeutic effect similar to that of PC in that it safeguards against aberrant changes in gait and alleviates knee edema.

RAR Decelerated Cartilage Degeneration and Enhanced ECM Anabolism in OA Rats

Micro-CT was performed to investigate further whether RAR has a protective effect on cartilage in the KOA model, and the data showed that the knee joints of the DMM group exhibited surface irregularity, fissures, and loss. The articular surface in the group treated with RAR and PC exhibited a smoother texture than that in the group subjected to DMM. In particular, the articular surface in the 600 mg/mL RAR-treated group was smoother, and subchondral bone sclerosis was less severe than that in the other groups (Figure 3A). As presented in Figures 3B–D, compared with those in the DMM group, the BV/TV and Tb.Th of subchondral bone were significantly greater in RAR and PC groups, but the Tb.Sp in RAR and PC groups was markedly lower. Figure 3B displays the BV/TV values. The DMM group had a considerably lower average BV/TV ratio (7.67 ± 2.36) than the sham group (26.0 ± 3.06). However, rats treated with 150, 300, and 600 mg/mL RAR and PC had BV/TV values of 13.33 ± 2.56, 19.0 ± 1.91, 20.17 ± 2.27, and 21.33 ± 3.14, respectively. RAR decreased bone degradation in vivo, as measured by BV/TV, Tb.Th, and Tb.Sp.

Proteoglycan depletion in keen cartilage was assessed using Safranin-O-solid green staining. Figure 3E illustrates that the DMM group had more severe articular cartilage injury and proteoglycan loss than the sham surgery group, suggesting that the DMM group's knee joint had greater cartilage damage. After treatment with RAR (150, 300, and 600 mg/mL) and PC for four weeks, cartilage damage and proteoglycan loss in the articular cartilage were alleviated compared to those in the DMM group. In particular, compared with the low-dose group, the 600 mg/mL RAR treatment group exhibited less cartilage damage and more proteoglycans. The Osteoarthritis Research Society International (OARSI) scores further confirmed this result (Figure 3F). Immunohistochemistry tests on knee joint samples were carried out to determine whether RAR slows OA development by delaying ECM breakdown in vitro (Figure 3E). Col2a1 and Acan protein expression were considerably lower in the DMM-induction group than in the sham group but increased in the DMM rats treated with RAR (150, 300, and 600 mg/mL) and PC. Furthermore, after four weeks, the anti-OA efficacy of 300 and 600 mg/mL RAR was superior to that of 150 mg/mL RAR (Figures 3G–H). These findings were verified by qRT-PCR (Figure 3I), indicating that RAR significantly slowed OA development in vivo by enhancing ECM formation.
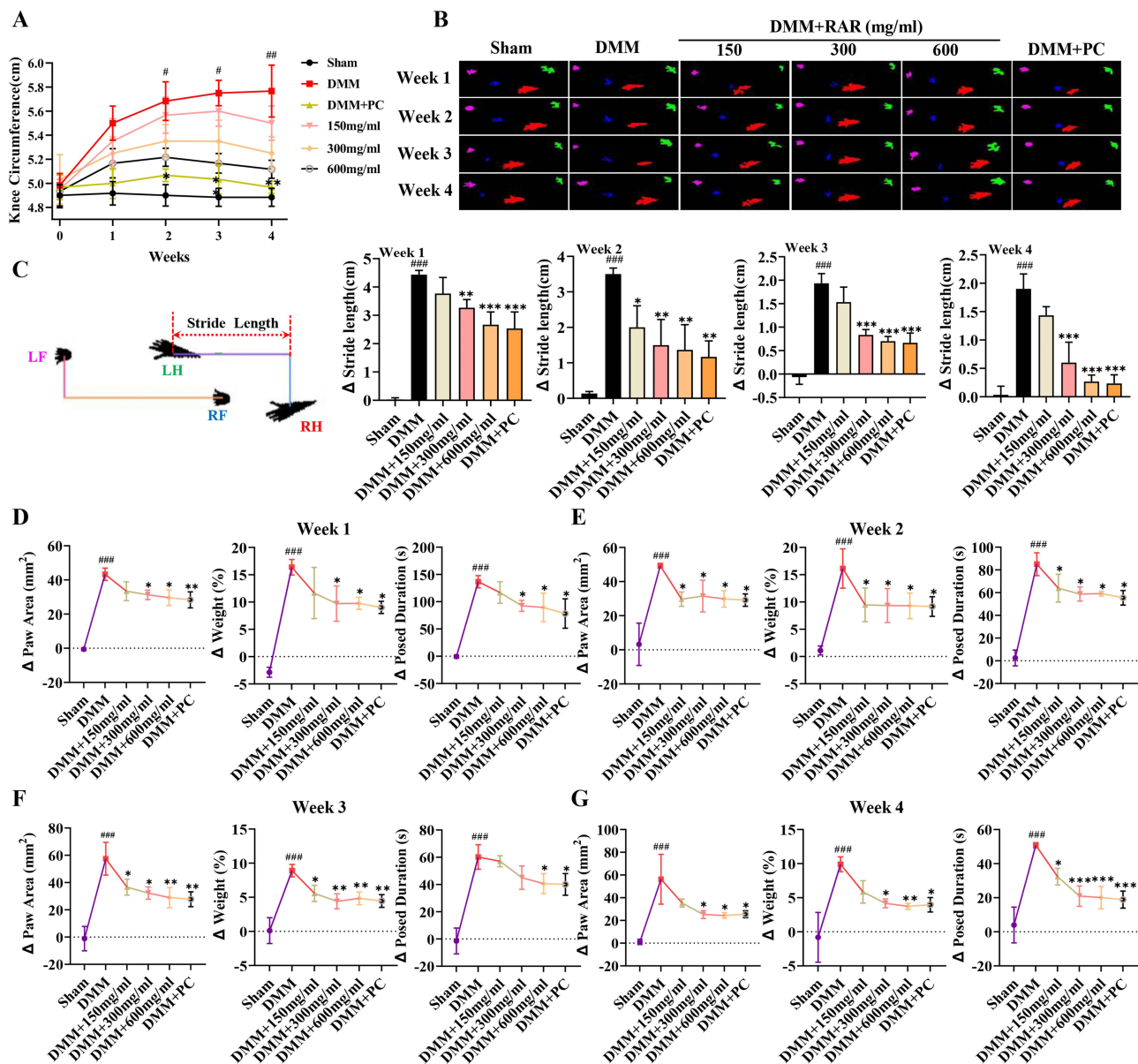
Figure 2 RAR ameliorates abnormal gait and swelling in OA rats. (**A**) Curve showing the degree of swelling of the right knee joint in the rats. (**B**) Rat gait imprint. (**C**) Changes in hind paw stride length of the rats. (**D–G**) Analysis of the paw area (mm³), paw weight (%), and exposure duration (s). All data are presented as the means ± standard deviations (n=10). Sham vs DMM, $^{###}P < 0.001$; DMM vs RAR/PC, $*P < 0.05$, $**P < 0.01$, $***P < 0.001$.

RAR Promotes Chondrocyte Anabolism and Inhibits Oxidative Stress in vitro

To determine the protective effect of RAR on cartilage, the optimal concentration of RAR for primary chondrocytes was initially determined using the CCK-8 assay. Figure 4A displays a statistically significant increase in cell viability when comparing 0.2 mg/mL at 24 h and 0.4 mg/mL at 48 h and 72 h to 0 mg/mL. Hence, for the subsequent experiments, concentrations of 0.1, 0.2, and 0.4 mg/mL were chosen. Following this, RAR application restored the glycosaminoglycan (GAG) loss in the cartilage matrix that was induced by IL-1β, as demonstrated by the Alcian blue staining results (Figure 4B). Additionally, the levels of Col2a1, Comp, and Acan, which are the primary constituents of cartilage, decreased significantly in response to IL-1β stimulation compared to those in the control group but increased in response to RAR treatment (Figure 4C). The results above indicate that RAR can increase ECM production by chondrocytes.
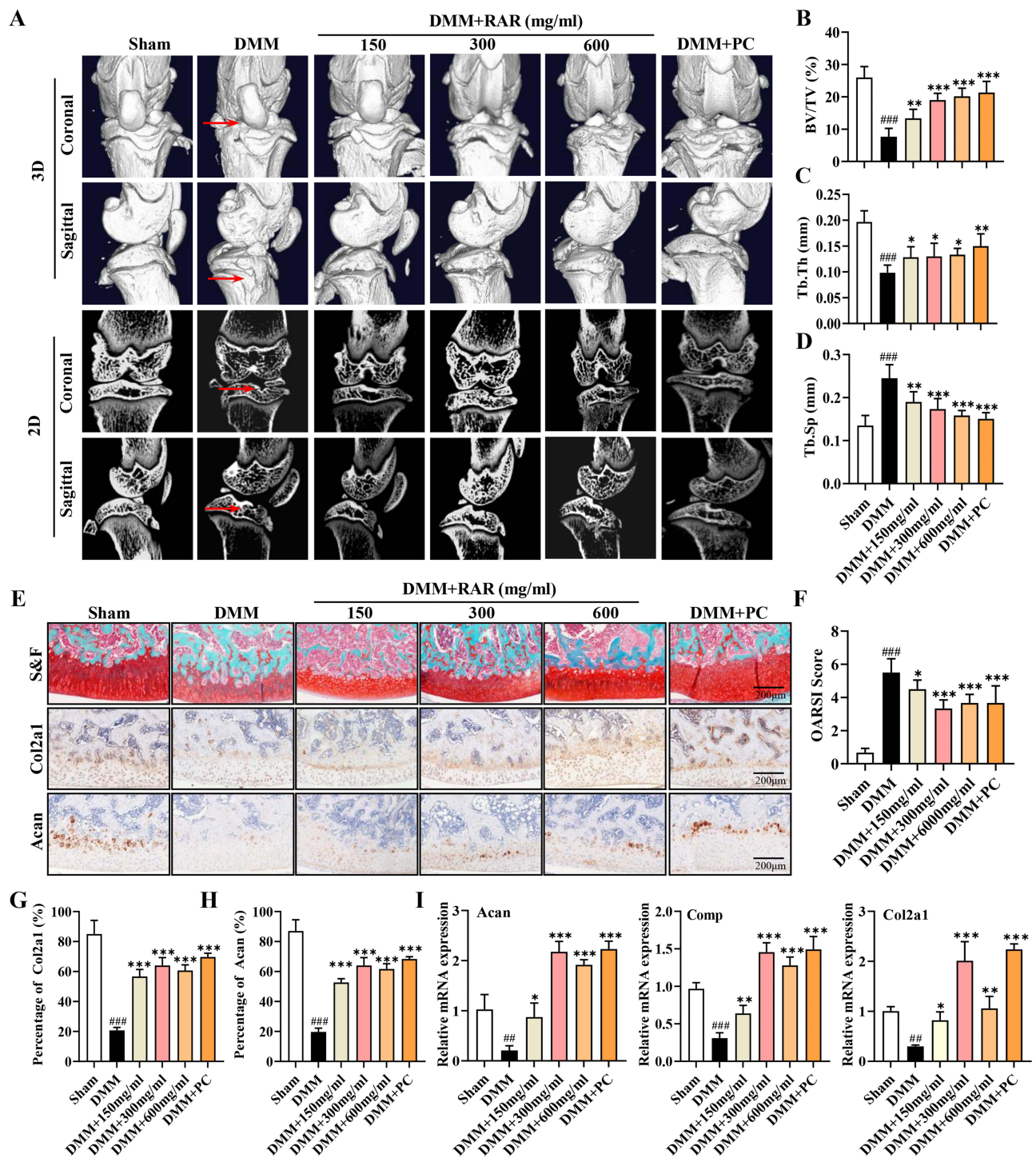
Figure 3 RAR decelerated cartilage degeneration and enhanced ECM anabolism in OA rats. (**A**) Rat knee joints scanned in 3D after RAR and PC therapy at several doses using Micro-CT. The red arrows indicate surface irregularities and cracks in the knee joints. (**B–D**) BV/TV, Tb.Th, and Tb.Sp quantitative analysis. (**E**) Rats' right knee joint stained with safranin-O-solid green (S&F). Col2a1 and Acan in cartilage stained with IHC. Scale bar=200 μm. (**F**) OARSI score of the tibial plateau. (**G** and **H**) Quantification of the percentage of positive expression of Col2a1 (%) and Acan (%). (**I**) Relative mRNA expression of Acan, Comp, and Col2a1 in DMM rats treated with RAR and PC. All data are presented as the means ± standard deviations (n=10). Sham vs DMM, $^{\#\#\#}P < 0.001$; DMM vs RAR/PC, $^{*}P < 0.05$, $^{**}P < 0.01$, $^{***}P < 0.001$.

Changes in antioxidant enzymes (SOD and GSH) indicate the presence of oxidative stress. SOD and GSH levels were lower in IL-1β-induced chondrocytes but considerably greater following RAR administration (Figure 4D). ROS are free radicals that are primarily produced by mitochondria, and their excessive synthesis is implicated in DNA damage in chondrocytes. Primary chondrocytes were pretreated at various concentrations (0.1, 0.2, and 0.4 mg/mL) before being
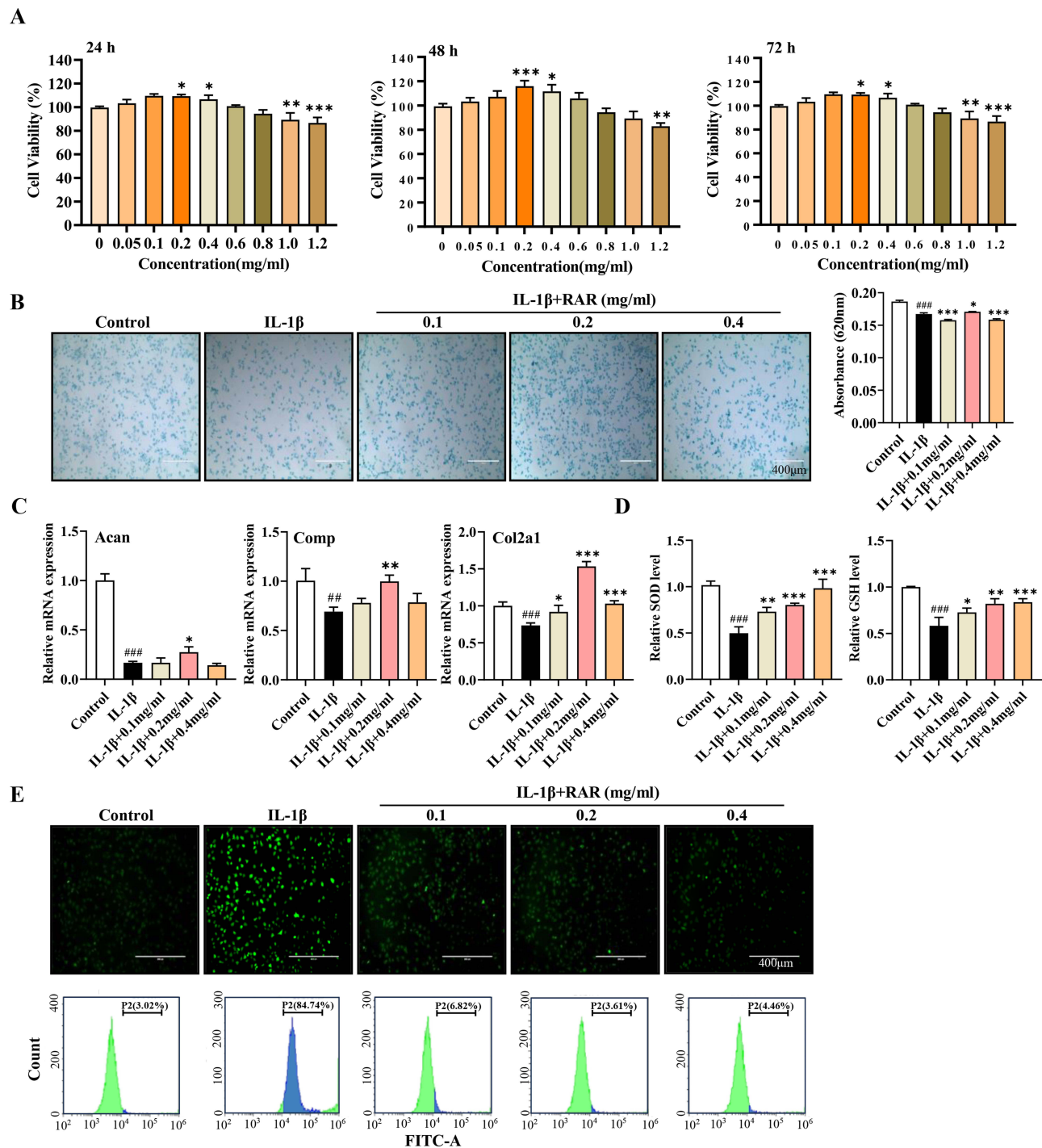
Figure 4 RAR promotes chondrocyte anabolism and inhibits oxidative stress in vitro. (**A**) CCK-8 was used to measure cell proliferation following 24, 48, and 72 h of RAR treatment. (**B**) Alcian blue staining was used to detect acidic polysaccharides at various RAR concentrations. (**C**) *Acan, Comp*, and *Col2a1* relative mRNA expression in IL-1β-induced primary chondrocytes treated with RAR. (**D**) Bar graph of SOD and GSH changes. (**E**) ROS generation in chondrocytes treated with various RAR concentrations was measured using the ROS probe DCFH-DA and quantified using a flow cytometer. Control vs IL-1β $^{\#\#}P < 0.01$, $^{\#\#\#}P < 0.001$; IL-1β vs RAR $*P < 0.05$, $** P < 0.01$, $*** P < 0.001$.

exposed to IL-1β (Figure 4E). Compared to the IL-1β group, the RAR-treated group exhibited a more substantial reduction in ROS levels, and the 0.2 mg/mL RAR-treated group exhibited the greatest anti-ROS effect. These data revealed that RAR has a significant antioxidative effect.

Screening of RAR Active Substances and KOA Therapeutic Targets

Network pharmacology was used to understand how RAR protects cartilage. First, 252 RAR-active chemicals were obtained from TCMSP. Using the oral bioavailability ≥ 30% and the drug-likeness ≥ 0.18 criteria, 17 active compounds were found after removing components with unexplored targets (Table 2). By scanning TCMSP and UniProt, 203 probable RAR active chemical targets and gene symbols were identified. The Cytoscape-based "Drug-Compound-Target" network had 223 nodes and 515 edges (Figure 5A). The DisGeNET, OMIM, DrugBank, GeneCards, and TTD databases yielded 2182 KOA-related target genes. The intersection of RAR drug targets and KOA disease targets included 119 common targets (Figure 5B).

Constructing the "Drug-Active Component-Target-Disease" Network and PPI Networks

Cytoscape software was used to construct a "drug-active component-target-disease" network to identify the linkages between RAR and their associated chemicals and KOA-shared targets. The results revealed 140 nodes and 399 edges, and the size of the quadrangle in the picture represents the degree value, with a larger size indicating increasing importance (Figure 6A). Network analysis revealed that quercetin, kaempferol, wogonin, baicalein, beta-sitosterol, and stigmasterol (99, 40, 32, 24, 20, and 12) had significantly higher degree value than the other compounds, suggesting that these six compounds may be the main active components for treating KOA. Subsequently, the content of six compounds were identified by HPLC-MS/MS analysis (Figure S1).

Next, a PPI network was created by importing 119 common targets into the String database. After deleting 16 disconnected nodes, 103 nodes and 469 edges remained (Figure 6B). The key targets of the genes were estimated by topological analysis using the following criteria: DC > 9, EC > 0.19, CC > 0.636, BC > 10.368, LAC > 5.159, and NC >6.496. As indicated in Figure 6C, *Jun, Rela, Tp53, Fos, Mapk1, Mapk14, Myc, Hif1A*, and *Esr1* were identified as the key gene targets involved in KOA pathogenesis.

Table 2 Active Compounds Contained in RAR

| Serial Number	Mol ID	Active Component	OB (%)	DL	Herb
SDH1	MOL000359	Sitosterol	36.91	0.75	Radix Rehmanniae Praeparata
NX1	MOL001458	Coptisine	30.67	0.86	Radix Achyranthis Bidentatae
NX2	MOL000173	Wogonin	30.68	0.23	Radix Achyranthis Bidentatae
NX3	MOL002714	Baicalein	33.52	0.21	Radix Achyranthis Bidentatae
NX4	MOL012461	28-norolean-17-en-3-ol	35.93	0.78	Radix Achyranthis Bidentatae
NX5	MOL001454	Berberine	36.86	0.78	Radix Achyranthis Bidentatae
NX6	MOL000085	Beta-daucosterol_qt	36.91	0.75	Radix Achyranthis Bidentatae
NX7	MOL002643	Delta 7-stigmastenol	37.42	0.75	Radix Achyranthis Bidentatae
NX8	MOL003847	Inophyllum E	38.81	0.85	Radix Achyranthis Bidentatae
NX9	MOL000422	Kaempferol	41.88	0.24	Radix Achyranthis Bidentatae
NX10	MOL001006	Poriferasta-7,22E-dien-3beta-ol	42.98	0.76	Radix Achyranthis Bidentatae
NX11	MOL004355	Spinasterol	42.98	0.76	Radix Achyranthis Bidentatae
NX12	MOL002897	Epiberberine	43.09	0.78	Radix Achyranthis Bidentatae
NX13	MOL000098	Quercetin	46.43	0.28	Radix Achyranthis Bidentatae
NX14	MOL000785	Palmatine	64.60	0.65	Radix Achyranthis Bidentatae
A1	MOL000449	Stigmasterol	43.83	0.76	Radix Rehmanniae Praeparata- Angelica Sinensis- Radix Achyranthis Bidentatae
B1	MOL000358	Beta-sitosterol	36.91	0.75	Angelica Sinensis-Radix Achyranthis Bidentatae
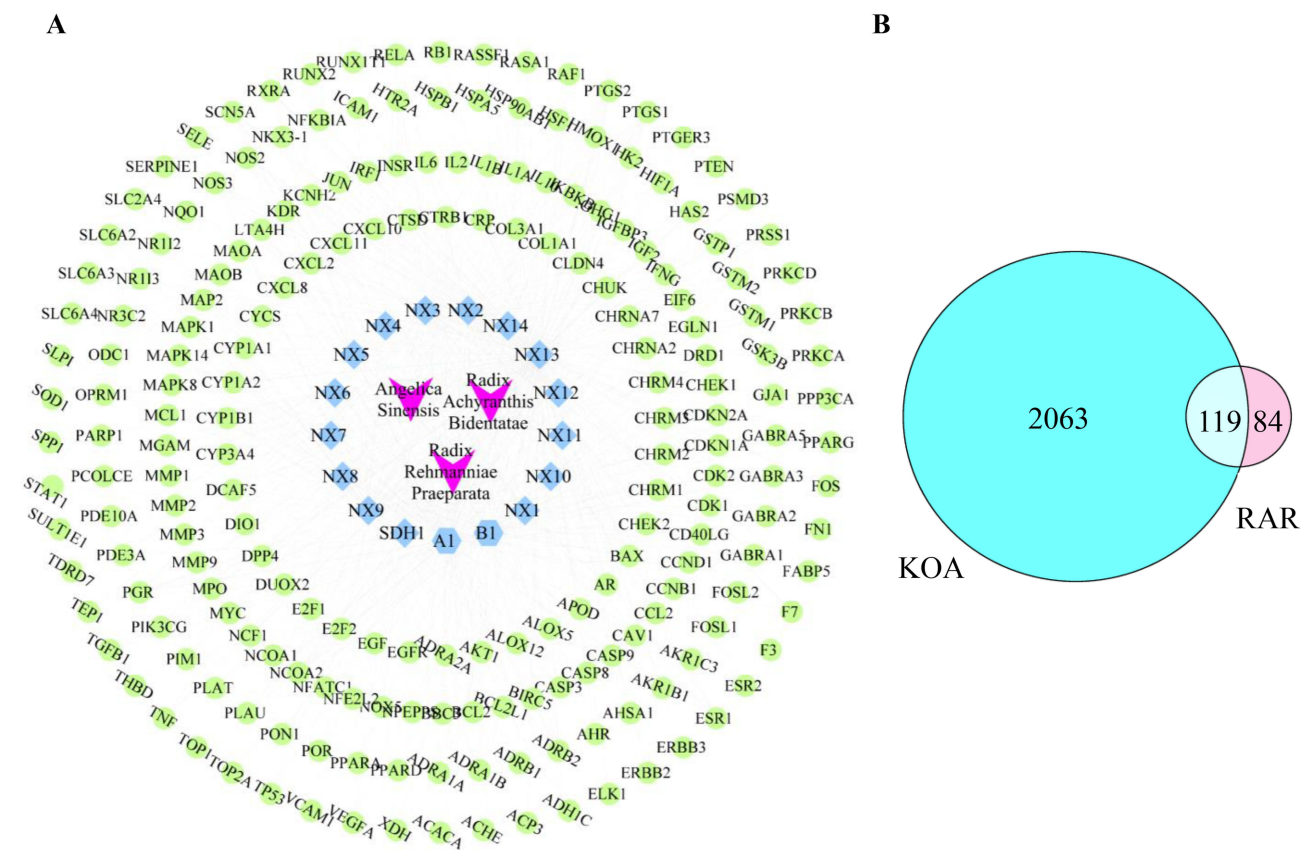
Figure 5 Target selection and network construction. (**A**) The "drug-compound-target" network of RAR. Green represents compound targets, light blue represents compounds in RAR, and purple represents drugs. (**B**) Common targets between RAR and KOA.

GO and KEGG Analysis

The nine key genes were imported into the Metascape database for GO and KEGG analyses to investigate the functional distribution of the gene targets for RAR therapy in KOA. A total of 202 GO terms were highly enriched ($P < 0.01$), with 181 related to biological processes (BP), 2 related to cell composition (CC), and 19 related to molecular function (MF). Figure 7A illustrates bar charts of the top ten enriched BP words, MF terms, and CC phrases. These findings suggest that several biological processes, including positive regulation of pri-miRNA transcription by RNA polymerase II, response to growth factor, cellular response to oxidative stress, aging, response to oxidative stress, and DNA-binding transcription factor binding, are involved in the anti-KOA effects of RAR. Similarly, the Metascape database was used to investigate KEGG pathway enrichment. The top 20 enriched pathways implicated in anti-KOA effects were evaluated, and the MAPK signaling pathway was shown to be significantly enriched (Figure 7B). The substantial enrichment in the MAPK signaling pathway in GO and KEGG databases suggested that RAR may treat KOA via this mechanism.

Results of Molecular Docking

Based on the findings of the "drug-active component-target-disease" network and PPI networks, the six primary compounds (quercetin, kaempferol, wogonin, baicalein, beta-sitosterol, and stigmasterol) were docked with their corresponding nine key genes (*Jun, Rela, Tp53, Fos, Mapk1, Mapk14, Myc, Hif1A*, and *Esr1*) (Table S1). PyMol software was employed to identify the compound target genes with < −5 kcal/mol binding energy scores together with their binding modes. As shown in Figure 8, the binding energies of Mapk1 with stigmasterol and beta-sitosterol are −7.54 and −5.41 kcal/mol, respectively; the binding energies of Jun with these two substances are −5.92 and −5.84 kcal/mol, respectively. Finally, Rela binds to beta-sitosterol with a binding energy of −5.43 kcal/mol. Thus, we speculate that *Rela, Jun*, and *Mapk1*, which are genes linked to the MAPK signaling pathway, could be the primary focal points of RAR treatment for KOA.
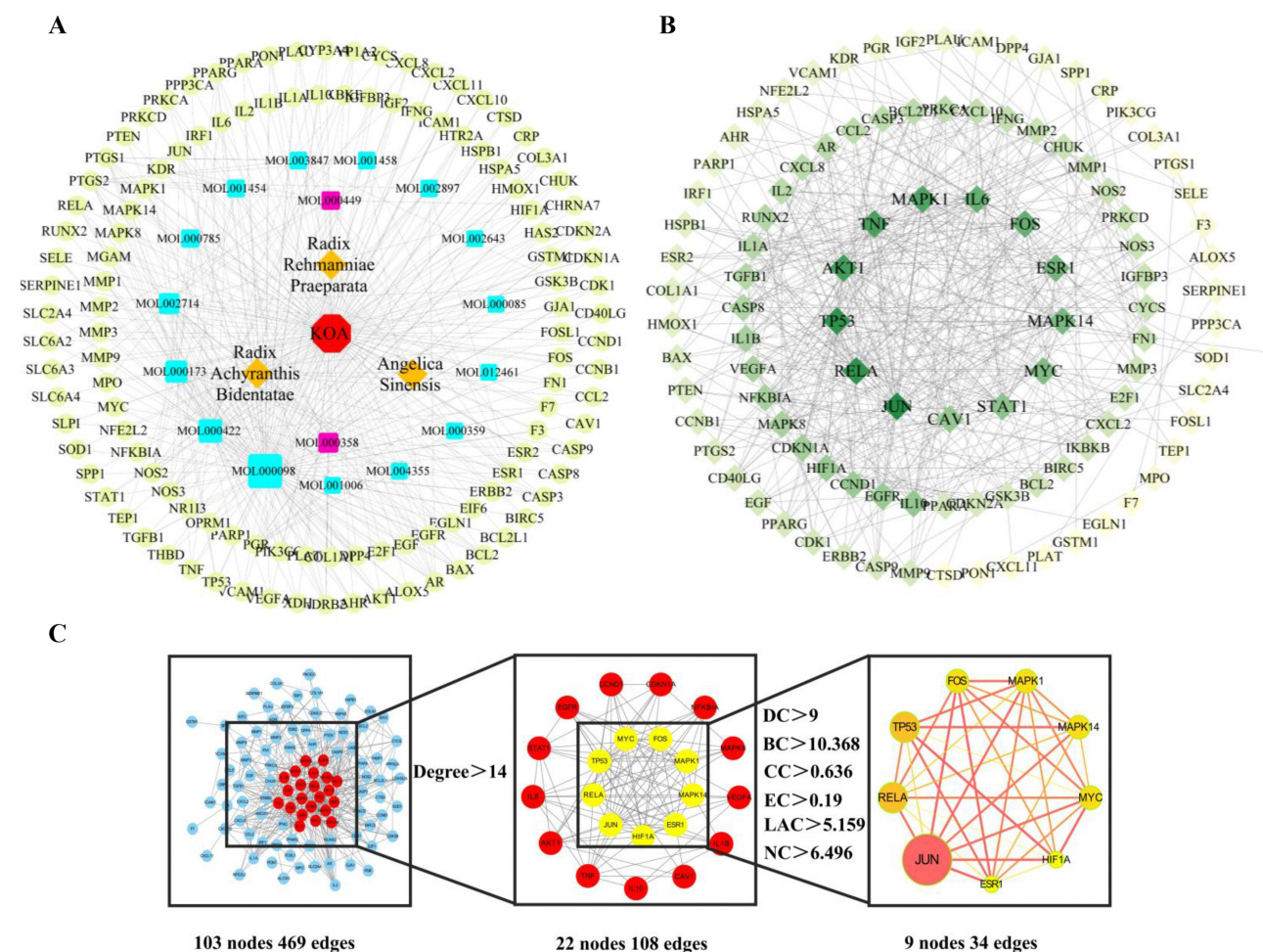
Figure 6 Construction of "drug-active component-target-disease" and PPI networks. (**A**) The "drug-active component-target-disease network". The red octagon represents disease, the blue quadrangle represents active compounds, the purple quadrangle represents common components, the yellow diamonds represent drugs, and the green circle represents compound targets. (**B**) PPI network of RAR-targeted common proteins for KOA therapy. The target proteins are shown as diamonds, with darker hues suggesting greater relevance. (**C**) The nine key RAR target genes for KOA. The size and color of the circle in the figure represent the degree value, and the thickness of the links between genes represents the combined score value.

Verification of the Mechanism by Which RAR Exerts Its Anti-KOA Effects

The genes (*Rela, Jun*, and *Mapk1*) within the MAPK signaling pathways were identified via qRT-PCR and IHC methods to confirm the network pharmacology findings. RAR therapy inhibited the significant increase in *Rela, Jun*, and *Mapk1* mRNA levels after IL-1β stimulation (Figure 9A). Similar trends in *Rela, Jun*, and *Mapk1* mRNA levels were observed in vivo (Figure 9B). Additionally, the expression level of Mapk1 was analyzed via IHC (Figure 9C). As expected, Mapk1 was consistently increased in DMM-induced OA model cartilage, and RAR treatment effectively suppressed this increase (Figure 9D). These findings indicate that RAR potentially governs the development of KOA by modulating MAPK signaling pathways (Figure 9E).

Discussion

KOA is a serious disorder that coexists with chronic inflammation and cartilage degradation, affecting the health and quality of life of the modern population.[35,36] Due to a number of risk factors, KOA not only affects the articular cartilage but also causes pathological alterations in the subchondral bone, ligaments, and periarticular muscles.[37,38] Consequently, there are currently no effective treatments for advanced KOA other than joint replacement, which represents a significant health obstacle for the future.[39] For thousands of years, TCM has been a vital element of complementary and alternative medicine, with a multitarget and multi-pathway impact on biology that is extensively employed in clinical settings.[40]
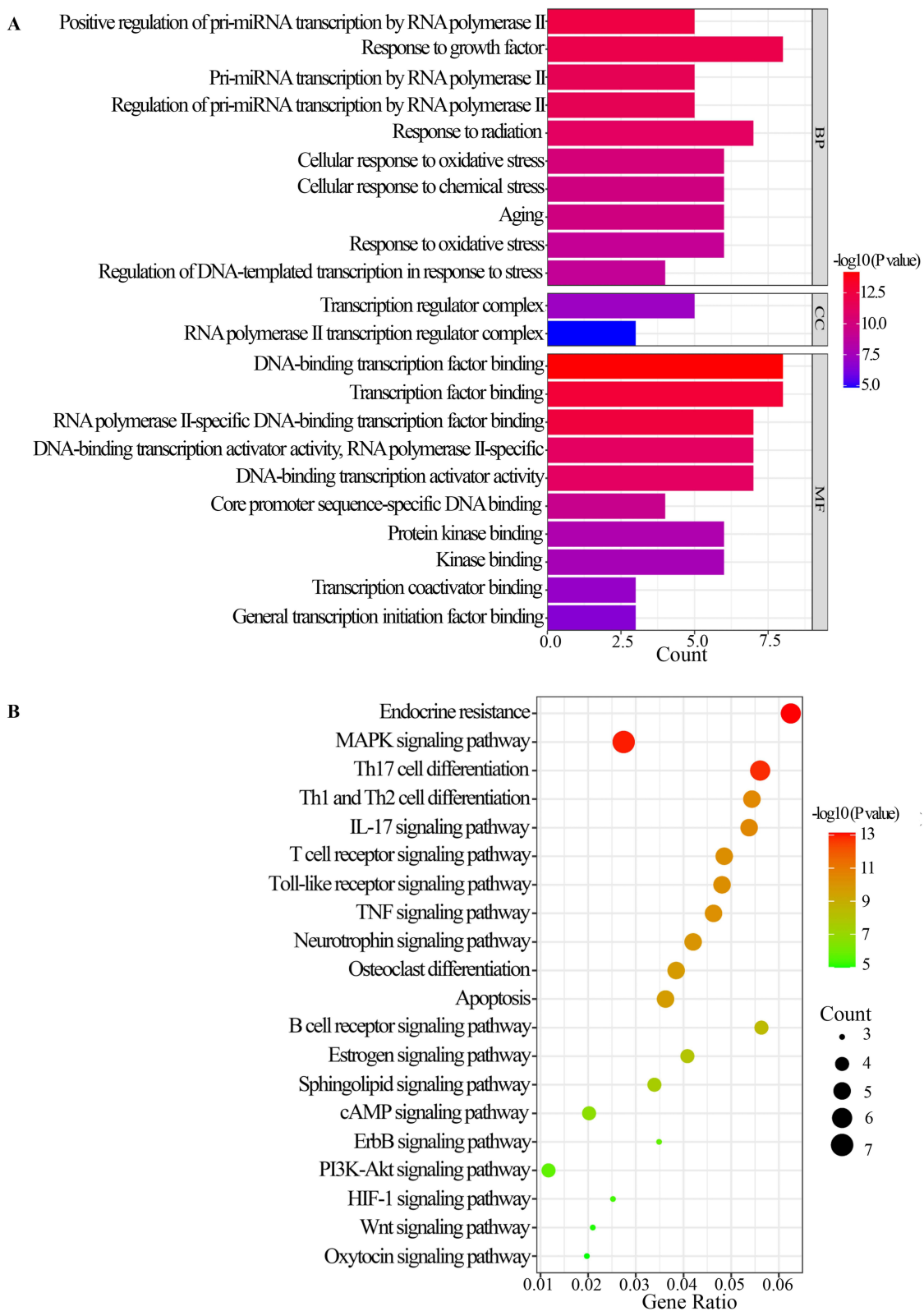
Figure 7 GO and KEGG analyses. (**A**) GO enrichment analysis. (**B**) KEGG pathway enrichment analysis.

Mapk1 with stigmasterol: -7.54 kcal/mol

Jun with stigmasterol: -5.92 kcal/mol

Jun with beta-sitosterol: -5.84 kcal/mol

Rela with beta-sitosterol: -5.43 kcal/mol
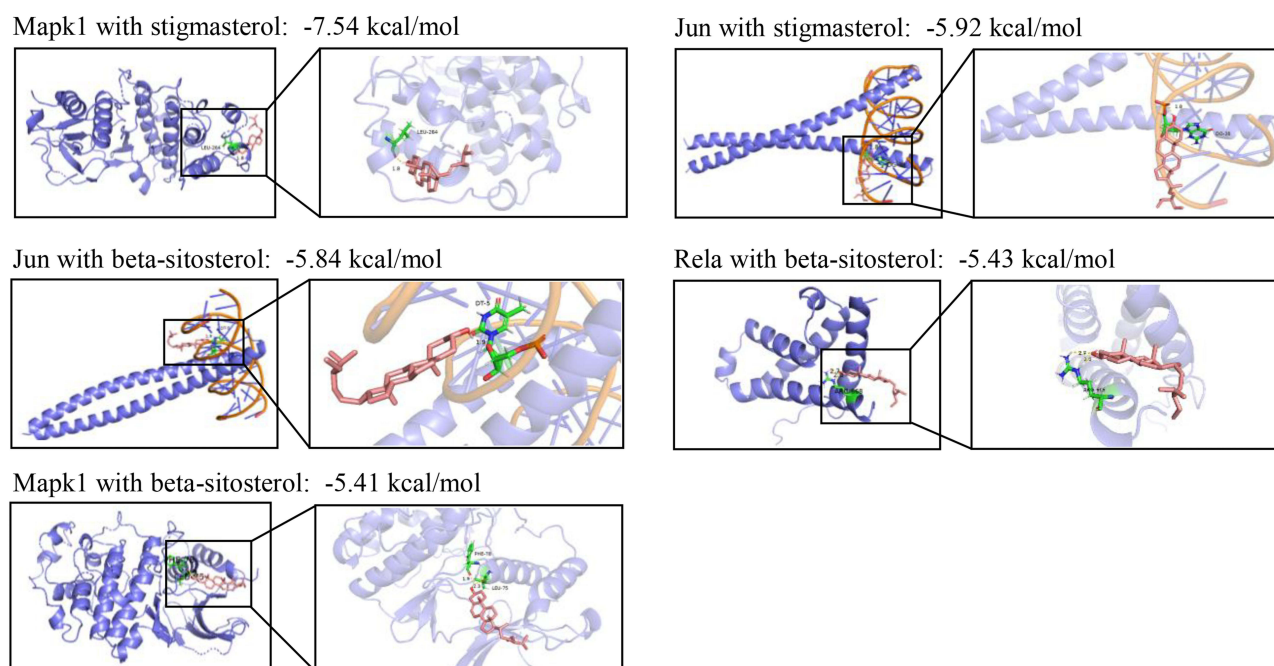
Mapk1 with beta-sitosterol: -5.41 kcal/mol

Figure 8 Molecular docking analysis. Molecular docking showed that stigmasterol and beta-sitosterol bind to Mapk1, Jun, and Rela.

The formula RAR comprises Radix Rehmanniae Preparata, Radix Angelicae Sinensis, and Radix Achyranthis Bidentatae. The three traditional Chinese herbs are widely used in the treatment of KOA, which served as the monarch drug in the efficacious formulations BSJGF and DHJST for KOA treatment, considering they exert significant therapeutic effects.[22,23] Previous study has reported that Radix Rehmanniae Preparata can inhibit bone resorption and balance the metabolism of articular cartilage via acting on proto-oncogene tyrosine-protein kinase Src. Moreover, Rehmanniae Radix Praeparata may exert anti-OA effect through other targets such as STAT3 and RELA, and other related pathways such as PI3K-AKT and IL-17 signaling pathways.[41] Catalpol is not only the main active component of Rehmannia glutinosa, but also its primary active component has been reported that can prevent IL-1β-induced chondrocyte injury through inhibiting the NF-κB pathway.[25] Glabralactone, a Coumarin Compound from Angelica Sinensis exhibited an anti-inflammatory activity in in vitro and in vivo through TRIF-Dependent IRF-3 signaling and NF- κB pathways.[26] Another study has shown the Angelica Sinensis polysaccharide has the ability to protect chondrocytes from H_2O_2-induced apoptosis via its antioxidant effects.[42] Radix Achyranthis Bidentatae is a Chinese traditional herbal medicine widely used to treat OA and Achyranthes bidentata polysaccharides could promote chondrocyte proliferation via activate the Wnt/β-catenin signaling pathway.[43] Thus, we speculation that RAR might have a therapeutic effect on OA. However, the bioactive chemical components and the mechanism behind the anti-KOA therapeutic effect of RAR are still unclear.

In this work, we investigated how RAR affects a DMM-induced KOA rat model and an IL-1β-induced OA chondrocyte model. The most evident clinical signs of KOA patients are limited knee joint motion, joint discomfort, and edema.[44] Interestingly, RAR improved knee joint function and reduced gait abnormalities and edema in KOA rats. In this study, we found that RAR might reduce substantial local articular cartilage degradation as well as the production of osteophytes in DMM-induced KOA rats. Inflammation may stimulate excessive catabolic processes in articular cartilage, leading to KOA development. RAR may inhibit articular cartilage ECM degradation by enhancing articular cartilage anabolism (Acan, Col2a1, and Comp). Increased ROS levels and reduced antioxidant activity have been identified in human OA cartilage, indicating that oxidative stress is a major cause of KOA onset and development.[45,46] To combat ROS-mediated damage, chondrocytes generate SOD and GSH, two major antioxidants.[47] According to Sun et al, IL-1β-mediated NADPH oxidase (Nox4) in chondrocyte metabolism might create excessive ROS, leading to matrix metalloproteinase-13 (MMP-13) release and articular cartilage breakdown.[48] Interestingly, treatment with RAR reversed the effects of IL-1β on the increase in ROS and decrease in SOD and GSH
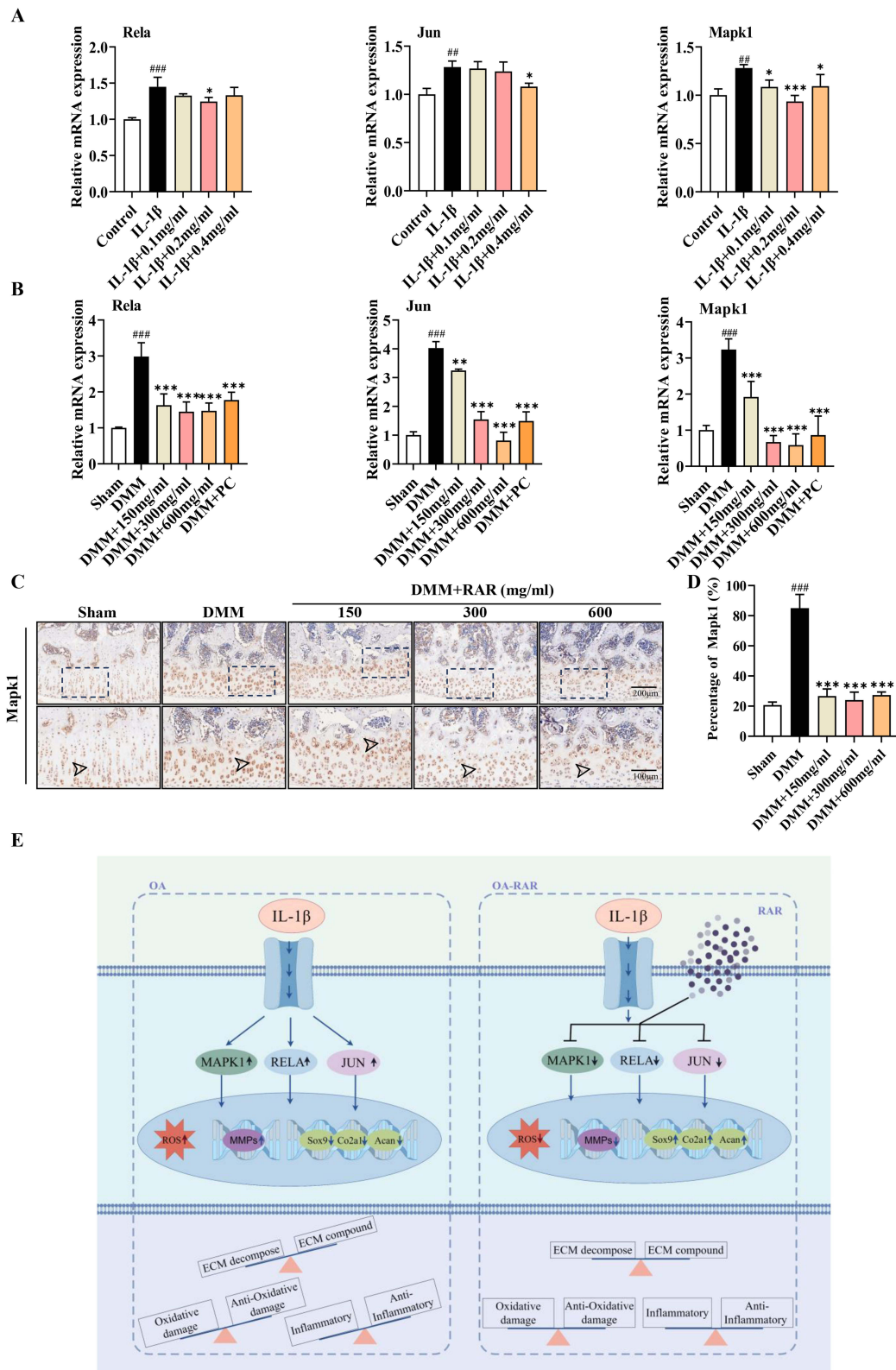
Figure 9 Verification of the mechanism by which RAR exerts its anti-KOA effects. (**A**) *Rela, Jun*, and *Mapk1* mRNA expression in IL-1β-induced primary chondrocytes treated with RAR. (**B**) *Rela, Jun*, and *Mapk1* mRNA expression in DMM rats treated with RAR and PC. (**C**) Cartilage-based Mapk1 IHC staining. Scale bar=200 μm. (**D**) Quantification of the percentage of positive expression of Mapk1 (%). (**E**) Schematic overview of mechanism was created by Figdraw. Control/Sham vs IL-1β/DMM $^{\#\#}$ $P <$ 0.01, $^{\#\#\#}P<$ 0.001; IL-1β/DMM vs RAR $*P <0.05$, $**P <0.01$, $***P <0.001$.

levels in chondrocytes. These findings confirmed the indispensability of RAR in the regulation of oxidative damage to articular cartilage.

To investigate the mechanism of RAR in the treatment of OA, network pharmacology was performed. A total of 119 potential RAR-KOA targets were identified. Based on the degree values in the "drug-active component-target-disease" network, the top 6 active RAR compounds (quercetin, kaempferol, wogonin, baicalein, beta-sitosterol and stigmasterol) were obtained. Quercetin possesses antioxidant and anti-inflammatory properties that may lower the production of inflammatory cytokines in joints and suppress the development of MMP-13 in chondrocytes, thereby protecting articular cartilage, reducing joint pain, and delaying the progression of KOA.[49,50] Pretreatment with kaempferol can effectively improve IL-1β-induced OA by suppressing inflammation, and has an obvious anti-inflammatory effect.[51,52] By decreasing chondrocyte apoptosis and the MAPK pathway, beta-sitosterol, one of the key components of the cell membrane, may decrease inflammation and cartilage deterioration in OA.[53,54] Stigmasterol can significantly attenuate cartilage degradation, DNA damage, mitochondrial dysfunction and ROS production, providing cartilage protection.[55]

With the use of bioinformatics, 9 key target genes were systematically attained. According to KEGG analysis, the target genes were mostly enriched in inflammatory and immune-related pathways, including TNF signaling, IL-1β, and MAPK and the MAPK signal pathway was the most abundant. The genes rich in the MAPK signal pathway were Mapk14, Fos, Jun, Myc, Mapk1, Rela and P53. To screen the key genes regulated by RAR, qRT-PCR analysis was performed and revealed that after the intervention of RAR, the expression of Mapk1, Jun and Rela genes in chondrocytes decreased significantly, but the other genes did not change significantly, suggesting that RAR primarily regulate Mapk1, Jun and Rela. Additionally, molecular docking analysis indicated that the active components beta-sitosterol and stigmasterol have good binding affinity to Mapk1, Jun and Rela. These results suggested that Mapk1, Jun and Rela are the key targets of RAR in the treatment of OA.

Studies have shown that Rela/p65 mediates the signal transduction of NF-κB and induces the transcription of Gremlin-1, thus inhibiting the expression of anabolic genes such as Sox9, Col2a1, and Acan, promoting the production of catabolic enzymes and inhibiting anabolism.[23,56,57] Studies have revealed that Jun can increase the expression of MMPs and decrease the synthesis of proteoglycans in chondrocytes. Inhibiting the Jnk-Jun axis can inhibit catabolism, promote anabolism, prevent chondrocytes from being ironed, maintain the normal composition of the extracellular matrix, protect chondrocytes, and delay OA progression.[58,59] Mapk1 is a subset of the MAPK family that controls several cellular processes, including cell growth, specialization, gene expression, and programmed cell death.[60] Reducing the level of Mapk1 can reduce the level of inflammation, inhibit catabolism, inhibit chondrocyte apoptosis, promote cartilage repair and delay the course of OA.[61]

To further validate the results of the molecular docking and KEGG analyses, we detected the levels of the key targets in vivo and in vitro and confirmed that Mapk1, Jun and Rela levels were significantly increased in DMM-induced rat articular cartilage and in IL-1β-induced chondrocytes; these effects could be reversed by RAR treatment. Taken together, RAR may exert anti-OA effect through the MAPK signal pathway and Mapk1, Jun and Rela may be the key targets. However, additional studies remain necessary to explicitly explain the specific mechanisms of *Mapk1* and explore the exact individual ingredients of RAR in KOA treatment.

Conclusion

In summary, we have integrated network pharmacological analysis and experimental evidence elucidated the RAR promoting the synthesis of articular cartilage ECM and reducing oxidative damage through regulating the MAPK signal pathway and Mapk1, Jun and Rela may be the key targets. Our study may provide new insights for the use of RAR in the therapy for KOA.

Abbreviations

KOA, Knee osteoarthritis; RAR, Radix Rehmanniae Praeparata- Angelica Sinensis-Radix Achyranthis Bidentatae; TCM, Traditional Chinese medicine; DMM, Destabilization of the medial meniscus model; ROS, Reactive oxygen species; SOD, Superoxide dismutase; GO, Gene ontology; KEGG, Kyoto Encyclopedia of genes and genomes; OA,

Osteoarthritis; NSAIDs, Nonsteroidal anti-inflammatory medicines; MAPK, Mitogen-activated protein kinase; TNF-α, Tumor necrosis factor-α; SOX9, SRY-related high mobility group box 9; MMP-13, Matrix metalloproteinase-13; BP, Biological process; CC, Cellular component.

Ethics Statement

All databases in this study are public databases, the contents of which are publicly available and allow unrestricted reuse through open licenses. According to the official document issued by the National Science and Technology Ethics Committee of China, the use of legally obtained public data is not subject to ethical scrutiny (https://www.gov.cn/zhengce/zhengceku/202302/28/content_5743658.htm). Therefore, for this study involving public databases, the need for ethics approval was waived (Ethics Committee of Changchun University of Chinese Medicine). All experimental animals survived at a constant temperature and humidity of 23 °C, with sufficient water and food, and a 12 h light/dark cycle. The pain of the rats was minimized during all surgical procedures. The animal studies were approved by the Animal Ethics Committee of Changchun University of Chinese Medicine (Application Number: 2024218) in accordance with the guidelines of the Guide for the Care and Use of Laboratory Animals.

Acknowledgments

Author Contributions

All authors made a significant contribution to the work reported, whether that is in the conception, study design, execution, acquisition of data, analysis and interpretation, or in all these areas. The authors participated in drafting, revising or critically reviewing the article. They provided final approval of the version to be published, agreed on the journal to which the article has been submitted, and agreed to be accountable for all aspects of the work. Wenhai Zhao is the first corresponding author, Haisi Dong is the second corresponding author.

Funding

Disclosure

The authors report no conflicts of interest in this work.

References

1. Sherwood J. Osteoarthritis year in review 2018: biology. *Osteoarthritis Cartilage*. 2019;27(3):365–370. doi:10.1016/j.joca.2018.10.005
2. Saengsiwaritt W, Ngamtipakon P, Udomsinprasert W. Vitamin D and autophagy in knee osteoarthritis: a review. *Int Immunopharmacol*. 2023;123:110712. doi:10.1016/j.intimp.2023.110712
3. Li M, Nie Y, Zeng Y, et al. The trajectories of depression symptoms and comorbidity in knee osteoarthritis subjects. *Clin Rheumatol*. 2022;41 (1):235–243. doi:10.1007/s10067-021-05847-9
4. Cui A, Li H, Wang D, Zhong J, Chen Y, Lu H. Global, regional prevalence, incidence and risk factors of knee osteoarthritis in population-based studies. *EClinicalMedicine*. 2020;29–30:100587. doi:10.1016/j.eclinm.2020.100587
5. Sellam J, Courties A, Eymard F, et al. Recommendations of the French society of rheumatology on pharmacological treatment of knee osteoarthritis. *Joint Bone Spine*. 2020;87(6):548–555. doi:10.1016/j.jbspin.2020.09.004
6. Rannou F, Pelletier JP, Martel-Pelletier J. Efficacy and safety of topical NSAIDs in the management of osteoarthritis: evidence from real-life setting trials and surveys. *Semin Arthritis Rheum*. 2016;45(4 Suppl):S18–21. doi:10.1016/j.semarthrit.2015.11.007
7. Xie Y, Zinkle A, Chen L, Mohammadi M. Fibroblast growth factor signalling in osteoarthritis and cartilage repair. *Nat Rev Rheumatol*. 2020;16 (10):547–564. doi:10.1038/s41584-020-0469-2

8. Liu R, Liu Z, Chen H, et al. Ginkgolide K delays the progression of osteoarthritis by regulating YAP to promote the formation of cartilage extracellular matrix. *Phytotherapy Res*. 2023;37:5205–5222. doi:10.1002/ptr.7953

9. Jin Y, Zhang Q, Qin X, et al. Carbon dots derived from folic acid attenuates osteoarthritis by protecting chondrocytes through NF-κB/MAPK pathway and reprogramming macrophages. *J Nanobiotechnol*. 2022;20(1):469. doi:10.1186/s12951-022-01681-6

10. Kapoor M, Martel-Pelletier J, Lajeunesse D, Pelletier JP, Fahmi H. Role of proinflammatory cytokines in the pathophysiology of osteoarthritis. *Nat Rev Rheumatol*. 2011;7(1):33–42. doi:10.1038/nrrheum.2010.196

11. Ingale D, Kulkarni P, Electricwala A, et al. Synovium-synovial fluid axis in osteoarthritis pathology: a key regulator of the cartilage degradation process. *Genes*. 2021;12(7):989. doi:10.3390/genes12070989

12. Zheng L, Zhang Z, Sheng P, Mobasheri A. The role of metabolism in chondrocyte dysfunction and the progression of osteoarthritis. *Ageing Res Rev*. 2021;66:101249. doi:10.1016/j.arr.2020.101249

13. Khan NM, Ahmad I, Haqqi TM. Nrf2/ARE pathway attenuates oxidative and apoptotic response in human osteoarthritis chondrocytes by activating ERK1/2/ELK1-P70S6K-P90RSK signaling axis. *Free Radic Biol Med*. 2018;116:159–171. doi:10.1016/j.freeradbiomed.2018.01.013

14. Xue S, Zhou X, Sang W, et al. Cartilage-targeting peptide-modified dual-drug delivery nanoplatform with NIR laser response for osteoarthritis therapy. *Bioact. Mater*. 2021;6(8):2372–2389. doi:10.1016/j.bioactmat.2021.01.017

15. Lepetsos P, Papavassiliou AG. ROS/oxidative stress signaling in osteoarthritis. *BBA*. 2016;1862(4):576–591. doi:10.1016/j.bbadis.2016.01.003

16. Lepetsos P, Papavassiliou KA, Papavassiliou AG. Redox and NF-κB signaling in osteoarthritis. *Free Radic Biol Med*. 2019;132:90–100. doi:10.1016/j.freeradbiomed.2018.09.025

17. Schieber M, Chandel NS. ROS function in redox signaling and oxidative stress. *Current Biology: CB*. 2014;24(10):R453–62. doi:10.1016/j.cub.2014.03.034

18. Ma JC, Luo T, Feng B, et al. Exploring the translational potential of PLGA nanoparticles for intra-articular rapamycin delivery in osteoarthritis therapy. *J Nanobiotechnol*. 2023;21(1):361. doi:10.1186/s12951-023-02118-4

19. Motta F, Barone E, Sica A, Selmi C. Inflammaging and Osteoarthritis. *Clin Rev All Immunol*. 2023;64(2):222–238. doi:10.1007/s12016-022-08941-1

20. Hosseinzadeh A, Kamrava SK, Joghataei MT, et al. Apoptosis signaling pathways in osteoarthritis and possible protective role of melatonin. *J Pinel Res*. 2016;61(4):411–425. doi:10.1111/jpi.12362

21. He Q, Yang J, Pan Z, et al. Biochanin A protects against iron overload associated knee osteoarthritis via regulating iron levels and NRF2/System xc-/GPX4 axis. *Biomed Pharmacothe*. 2023;157:113915. doi:10.1016/j.biopha.2022.113915

22. Chen WJ, Zhuang Y, Peng W, Cui W, Zhang SJ, Wang JW. Du Huo Ji Sheng Tang inhibits Notch1 signaling and subsequent NLRP3 activation to alleviate cartilage degradation in KOA mice. *ChinMed*. 2023;18(1):80. doi:10.1186/s13020-023-00784-y

23. Zhou Z, Lv C, Wang Y, et al. BuShen JianGu Fang alleviates cartilage degeneration via regulating multiple genes and signaling pathways to activate NF-κB/Sox9 axis. *Phytomedicine*. 2023;113:154742. doi:10.1016/j.phymed.2023.154742

24. Jhun JY, Na HS, Shin JW, et al. Notoginseng radix and rehmanniae radix preparata extract combination (YH23537) reduces pain and cartilage degeneration in rats with monosodium iodoacetate-induced osteoarthritis. *J Med Food*. 2018;21(8):745–754. doi:10.1089/jmf.2017.4041

25. Pang Y, Zhao L, Ji X, Guo K, Yin X. Analyses of transcriptomics upon IL-1β-stimulated mouse chondrocytes and the protective effect of catalpol through the NOD2/NF-κB/MAPK signaling pathway. *Molecules*. 2023;28(4):1606. doi:10.3390/molecules28041606

26. Choi TJ, Song J, Park HJ, Kang SS, Lee SK. Anti-inflammatory activity of glabralactone, a coumarin compound from angelica sinensis, via suppression of TRIF-Dependent IRF-3 signaling and NF-κB pathways. *Mediators Inflam*. 2022;2022:5985255. doi:10.1155/2022/5985255

27. Xu C, Ni S, Zhuang C, et al. Polysaccharide from Angelica sinensis attenuates SNP-induced apoptosis in osteoarthritis chondrocytes by inducing autophagy via the ERK1/2 pathway. *Arthritis Res Therap*. 2021;23(1):47. doi:10.1186/s13075-020-02409-3

28. Hyun SW, Lee TG, Song SJ, Kim CS. Evaluation of oral toxicity and genotoxicity of Achyranthis Radix extract. *J Ethnopharmacol*. 2021;274:113944. doi:10.1016/j.jep.2021.113944

29. Yuan H, Ma Q, Cui H, et al. How Can synergism of traditional medicines benefit from network pharmacology? *Molecules*. 2017;22(7):1.

30. Liu J, Liu J, Tong X, et al. Network pharmacology prediction and molecular docking-based strategy to discover the potential pharmacological mechanism of huai hua san against ulcerative colitis. *Drug Des Devel Ther*. 2021;15:3255–3276. doi:10.2147/dddt.S319786

31. Bannuru RR, Osani MC, Vaysbrot EE, et al. OARSI guidelines for the non-surgical management of knee, Hip, and polyarticular osteoarthritis. *Osteoarthritis Cartilage*. 2019;27(11):1578–1589. doi:10.1016/j.joca.2019.06.011

32. Glasson SS, Blanchet TJ, Morris EA. The surgical destabilization of the medial meniscus (DMM) model of osteoarthritis in the 129/SvEv mouse. *Osteoarthritis Cartilage*. 2007;15(9):1061–1069. doi:10.1016/j.joca.2007.03.006

33. Zhou Z, Zhong J, Zhang J, et al. Comparative transcriptome analysis provides insight into the molecular targets and signaling pathways of deer TGF-1 regulating chondrocytes proliferation and differentiation. *Molecular Biology Reports Apr*. 2023;50(4):3155–3166. doi:10.1007/s11033-023-08265-z

34. Bao J, Lin C, Zhou X, et al. circFAM160A2 promotes mitochondrial stabilization and apoptosis reduction in osteoarthritis chondrocytes by targeting miR-505-3p and SIRT3. *Oxid Med Cell Longev*. 2021;2021:5712280. doi:10.1155/2021/5712280

35. Gao XR, Chen YS, Deng W. The effect of vitamin D supplementation on knee osteoarthritis: a meta-analysis of randomized controlled trials. *Intl j Surgery*. 2017;46:14–20. doi:10.1016/j.ijsu.2017.08.010

36. Moretti L, Bizzoca D, Geronimo A, et al. towards precision medicine for osteoarthritis: focus on the synovial fluid proteome. *Int J Mol Sci*. 2022;23(17):9731. doi:10.3390/ijms23179731

37. Muthu S, Korpershoek JV, Novais EJ, Tawy GF, Hollander AP, Martin I. Failure of cartilage regeneration: emerging hypotheses and related therapeutic strategies. *Nat Rev Rheumatol*. 2023;19(7):403–416. doi:10.1038/s41584-023-00979-5

38. Ansari MY, Ahmad N, Haqqi TM. Oxidative stress and inflammation in osteoarthritis pathogenesis: role of polyphenols. *Biomed Pharmacothe*. 2020;129:110452. doi:10.1016/j.biopha.2020.110452

39. Latourte A, Kloppenburg M, Richette P. Emerging pharmaceutical therapies for osteoarthritis. *Nat Rev Rheumatol*. 2020;16(12):673–688. doi:10.1038/s41584-020-00518-6

40. Shi Q, Huang L, Duan J, Kuang G, Lu M, Tan X. The effects of Jiawei Duhuo Jisheng mixture on Wnt/β-catenin signaling pathway in the synovium inflamed by knee osteoarthritis: an in vitro and in vivo experiment. *J Ethnopharmacol*. 2022;294:115363. doi:10.1016/j.jep.2022.115363

41. Feng WQ, Liu KY, Zhang JN, et al. Study on mechanism of Rehmanniae Radix Praeparata for treatment of osteoarthritis based on network pharmacology and molecular docking. *Zhongguo Zhong Yao Za Zhi*. 2022;47(19):5336–5343. doi:10.19540/j.cnki.cjcmm.20220427.401

42. Zhuang C, Ni S, Yang ZC, Liu RP. Oxidative stress induces chondrocyte apoptosis through caspase-dependent and caspase-independent mitochondrial pathways and the antioxidant mechanism of angelica sinensis polysaccharide. *Oxid Med Cell Longev.* 2020;2020:3240820. doi:10.1155/2020/3240820

43. Weng X, Lin P, Liu F, et al. Achyranthes bidentata polysaccharides activate the Wnt/beta-catenin signaling pathway to promote chondrocyte proliferation. *Int J Mol Med.* 2014;34(4):1045–1050. doi:10.3892/ijmm.2014.1869

44. Pogonchenkova I, Uyanayeva A, Tupitsyna Y, et al. [Meteocorrective effect of physical and balneal factors in patients with joint diseases]. *Voprosy Kurortologii, Fizioterapii, i Lechebnoi Fizicheskoi Kultury.* 2022;99(4):5–12. Russian. doi:10.17116/kurort2022990415

45. Liu L, Luo P, Yang M, Wang J, Hou W, Xu P. The role of oxidative stress in the development of knee osteoarthritis: a comprehensive research review. *Front Mol Biosci.* 2022;9:1001212. doi:10.3389/fmolb.2022.1001212

46. Bolduc JA, Collins JA, Loeser RF. Reactive oxygen species, aging and articular cartilage homeostasis. *Free Radic Biol Med.* 2019;132:73–82. doi:10.1016/j.freeradbiomed.2018.08.038

47. Amirkhizi F, Ghoreishy SM, Baker E, Hamedi-Shahraki S, Asghari S. The association of vitamin D status with oxidative stress biomarkers and matrix metalloproteinases in patients with knee osteoarthritis. *Front Nutri.* 2023;10:1101516. doi:10.3389/fnut.2023.1101516

48. Li X, Fu X, Li H, et al. Leptin accelerates BMSC transformation into vertebral epiphyseal plate chondrocytes by activating SENP1-mediated deSUMOylation of SIRT3. *FEBS Open Bio.* 2023;13(2):293–306. doi:10.1002/2211-5463.13539

49. Wang Q, Ying L, Wei B, Ji Y, Xu Y. Effects of quercetin on apoptosis and extracellular matrix degradation of chondrocytes induced by oxidative stress-mediated pyroptosis. *J Biochem Mol Toxi.* 2022;36(2):e22951. doi:10.1002/jbt.22951

50. Lv S, Wang X, Jin S, Shen S, Wang R, Tong P. Quercetin mediates TSC2-RHEB-mTOR pathway to regulate chondrocytes autophagy in knee osteoarthritis. *Gene.* 2022;820:146209. doi:10.1016/j.gene.2022.146209

51. Xiao Y, Liu L, Zheng Y, Liu W, Xu Y. Kaempferol attenuates the effects of XIST/miR-130a/STAT3 on inflammation and extracellular matrix degradation in osteoarthritis. *Future Med Chem.* 2021;13(17):1451–1464. doi:10.4155/fmc-2021-0127

52. Estakhri F, Panjehshahin MR, Tanideh N, et al. The effect of kaempferol and apigenin on allogenic synovial membrane-derived stem cells therapy in knee osteoarthritic male rats. *The Knee.* 2020;27(3):817–832. doi:10.1016/j.knee.2020.03.005

53. Cheng BC, Fu XQ, Guo H, et al. The genus Rosa and arthritis: overview on pharmacological perspectives. *Pharmacol Res.* 2016;114:219–234. doi:10.1016/j.phrs.2016.10.029

54. Lou C, Lin C, Wang W, et al. Extracts of Oldenlandia diffusa protects chondrocytes via inhibiting apoptosis and associated inflammatory response in osteoarthritis. *J Ethnopharmacol.* 2023;316:116744. doi:10.1016/j.jep.2023.116744

55. Haque MN, Hannan MA, Dash R, Choi SM, Moon IS. The potential LXRβ agonist stigmasterol protects against hypoxia/reoxygenation injury by modulating mitophagy in primary hippocampal neurons. *Phytomedicine.* 2021;81:153415. doi:10.1016/j.phymed.2020.153415

56. Chang SH, Mori D, Kobayashi H, et al. Excessive mechanical loading promotes osteoarthritis through the gremlin-1-NF-κB pathway. *Nat Commun.* 2019;10(1):1442. doi:10.1038/s41467-019-09491-5

57. Kobayashi H, Chang SH, Mori D, et al. Biphasic regulation of chondrocytes by Rela through induction of anti-apoptotic and catabolic target genes. *Nat Commun.* 2016;7:13336. doi:10.1038/ncomms13336

58. He T, Wu D, He L, et al. Casein kinase 1 epsilon facilitates cartilage destruction in osteoarthritis through JNK pathway. *FASEB j.* 2020;34 (5):6466–6478. doi:10.1096/fj.201902672R

59. Ge HX, Zou FM, Li Y, Liu AM, Tu M. JNK pathway in osteoarthritis: pathological and therapeutic aspects. *J Receptor Signal Trans Res.* 2017;37 (5):431–436. doi:10.1080/10799893.2017.1360353

60. Li Z, Dai A, Yang M, Chen S, Deng Z, Li L. p38MAPK signaling pathway in osteoarthritis: pathological and therapeutic aspects. *J Inflamm Res.* 2022;15:723–734. doi:10.2147/jir.S348491

61. Jiang T, Gong Y, Zhang W, et al. PD0325901, an ERK inhibitor, attenuates RANKL-induced osteoclast formation and mitigates cartilage inflammation by inhibiting the NF-κB and MAPK pathways. *Bioorg Chem.* 2023;132:106321. doi:10.1016/j.bioorg.2022.106321